Anal. Chem. **2004,** *76,* 5257−5264

Microfluidic Shear Devices for Quantitative Analysis of Cell Adhesion

Hang Lu,[†,‡,§] Lily Y. Koo,[†,‡,∥] Wechung M. Wang,[†] Douglas A. Lauffenburger,[†,⊥] Linda G. Griffith,[⊥,#] and Klavs F. Jensen*[,†]

Department of Chemical Engineering, Division of Biological Engineering, and Biotechnology Process Engineering Center, and Department of Mechanical Engineering, Massachusetts Institute of Technology, Cambridge, Massachusetts 02139

We describe the design, construction, and characterization of microfluidic devices for studying cell adhesion and cell mechanics. The method offers multiple advantages over previous approaches, including a wide range of distractive forces, high-throughput performance, simplicity in experimental setup and control, and potential for integration with other microanalytic modules. By manipulating the geometry and surface chemistry of the microdevices, we are able to vary the shear force and the biochemistry during an experiment. The dynamics of cell detachment under different conditions can be captured simultaneously using time-lapse videomicroscopy. We demonstrate assessment of cell adhesion to fibronectin-coated substrates as a function of the shear stress or fibronectin concentration in microchannels. Furthermore, a combined perfusion-shear device is designed to maintain cell viability for long-term culture as well as to introduce exogenous reagents for biochemical studies of cell adhesion regulation. In agreement with established literature, we show that fibroblasts cultured in the combined device reduced their adhesion strength to the substrate in response to epidermal growth factor stimulation.

Adhesive interactions between cells and their physical environments are central in developmental biology, tissue maintenance, tissue engineering, cancer progression, and biotechnological processes. Several methods have been developed to measure cell−substrate adhesion strength through the application of distractive forces to adherent cells. These adhesion assays can be classified according to the nature of the distractive force applied: hydrodynamic shear force,[1,2] centrifugal (normal) force,[3,4] and micromanipulation.[5,6] However, the limitations of these currently available assays include low-throughput performance, cumbersome apparatus assembly, apparatus failure, and inadequate range of detachment forces. For example, the centrifugation assay can measure multiple cellular or biochemical events, but only one constant normal force can be applied in one run, and the magnitude of the force is severely constrained by equipment safety requirements. In contrast, variations in surface biochemical properties and cell types are limited in shear force-based assays that use chamber geometry to generate variable shear force. An alternative approach assesses single-cell adhesion properties using micropipets or force-responsive microprobes. These micromanipulation experiments, while revealing features of individual cell behavior, are technique-intensive, low-throughput, and laborious if statistical results for a cell population as a whole are desired. To address some of the limitations faced by the conventional methods, we have designed a series of simple microfluidic devices fabricated using the rapid prototyping techniques.[7]

Microfluidic chips have emerged as a means to improve throughput, resolution, and fidelity of measurements in many biological applications.[8−11] In this work, we show that microfluidic systems also offer unique advantages in quantitative cell adhesion studies. The small dimensions associated with micrometer-sized channels ensure laminar flow even at very high linear fluid velocities, which are often required when large shear stresses are generated. This is an important feature because many of the existing adhesion assays are limited by the achievable range of applied forces. In addition, the microfluidic devices only require a small amount of reagents. These devices can be operated readily in parallel for high-throughput experimentation compared to the conventional methods.

* Author to whom correspondence should be addressed. Phone: 617-253-4589. Fax: 617-258-8224. E-mail: kfjensen@mit.edu.

[†] Department of Chemical Engineering.

[‡] These authors contributed equally.

[§] Present address: 513 Parnassus Ave., Rm S-1471, UCSF Department of Anatomy, Box 0452, San Francisco, CA 94143-0452.

[∥] Present address: NIAID/NIH, 10 Center Dr., Bldg 10 Rm 11N308, Bethesda, MD 20892.

[⊥] Division of Biological Engineering, and Biotechnology Process Engineering Center.

[#] Department of Mechanical Engineering.

(1) Garcia, A. J.; Ducheyne, P.; Boettiger, D. *Biomaterials* **1997**, *18*, 1091−1098.

(2) Usami, S.; Chen, H. H.; Zhao, Y. H.; Chien, S.; Skalak, R. *Ann. Biomed. Eng.* **1993**, *21*, 77−83.

(3) McClay, D. R.; Wessel, G. M.; Marchase, R. B. *Proc. Natl. Acad. Sci. U.S.A.* **1981**, *78*, 4975−4979.

(4) Chu, L.; Tempelman, L. A.; Miller, C.; Hammer, D. A. *AIChE J.* **1994**, *40*, 692−703.

(5) Tozeren, A.; Sung, K. L. P.; Sung, L. A.; Dustin, M. L.; Chan, P. Y.; Springer, T. A.; Chien, S. *J. Cell Biol.* **1992**, *116*, 997−1006.

(6) Merkel, R.; Nassoy, P.; Leung, A.; Ritchie, K.; Evans, E. *Nature* **1999**, *397*, 50−53.

(7) Duffy, D. C.; McDonald, J. C.; Schueller, O. J. A.; Whitesides, G. M. *Anal. Chem.* **1998**, *70*, 4974−4984.

(8) Burns, M. A.; Johnson, B. N.; Brahmasandra, S. N.; Handique, K.; Webster, J. R.; Krishnan, M.; Sammarco, T. S.; Man, P. M.; Jones, D.; Heldsinger, D.; Mastrangelo, C. H.; Burke, D. T. *Science* **1998**, *282*, 484−487.

(9) Fu, A. Y.; Spence, C.; Scherer, A.; Arnold, F. H.; Quake, S. R. *Nat. Biotechnol.* **1999**, *17*, 1109−1111.

(10) Santini, J. T.; Cima, M. J.; Langer, R. *Nature* **1999**, *397*, 335−338.

(11) Weigl, B. H.; Yager, P. *Science* **1999**, *283*, 346−347.

10.1021/ac049837t CCC: $27.50
Published on Web 08/17/2004

The rapid prototyping technique with poly(dimethylsiloxane) (PDMS) imparts additional benefits by ensuring a fast turnaround time for device design, fabrication, and testing. PDMS, being optically transparent, enables the use of different real-time microscopy techniques to explore cell behaviors under diverse experimental conditions. In this work, we used time-lapse video-microscopy to capture the dynamics of cell detachment under multiple conditions simultaneously.

Using the microfluidic devices, we assessed short-term cell adhesion as a function of the surface density of adhesion molecules, shear stress, and cell type. We also introduced microfluidic devices designed to allow long-term culture of mammalian cells and introduction of exogenous reagents through continuous perfusion. As an example of the utility of these devices in addressing biologically relevant phenomena, we probed the effect of epidermal growth factor (EGF) on long-term cell adhesion. Our results obtained using the microfluidic assay device are in agreement with those obtained previously using the traditional assays.[12,13]

EXPERIMENTAL SECTION

Fluid Dynamics in Microdevices and Forces on Adherent Cells. To design and characterize the microfluidic devices of interest, we first used the simple Poiseuille model to explore the design space and determine the experimental regimes. This model assumes parallel plate configuration with infinite aspect ratio in the cross-sectional dimensions. The shear stress, τ, and pressure drop, ΔP, are functions of volumetric flow rate, Q, channel dimensions (height, h, width, w, and length, L), and fluid viscosity, μ, as follows,

$$\tau = -(12Q\mu/h^2w) \quad (1)$$

$$\Delta P/L = -(12Q\mu/h^3w) \quad (2)$$

Calculation of the Reynolds number, $Re = uh\rho/\mu$, allowed determination of wall and entrance effects within the microchannels (where the average linear velocity, u, is calculated from the volumetric flow rate as $u = Q/hw$).[14] Shear stresses and pressure drops were also calculated using the analytical solution for rectangular channel flow[15] to evaluate the accuracy of the simple Poiseuille model. Details of this analysis are included in the Appendix.

Finally, computational fluid dynamic software (CFD-ACE+, Huntsville, AL) was used to construct three-dimensional (3-D) models that emulate either a flat cell or a dome-shaped cell, to understand the influence of surface topology, as introduced by the presence of adherent cells, in shear stress determination. The model assumes symmetry and used only half of a biological cell inside the computational domain. Experimental observations were used as guidelines for determining cellular parameters for this model. Specifically, the fibroblast cells used in this study were ~11 μm in diameter in suspension and spread to ~20 μm in diameter shortly after attachment. When modeling a spread cell as a dome, the radius of curvature and the height of the dome were determined by assuming conservation of the cell volume. In the model, 4 μm was used as the dome height. The entire computation domain was 60 μm long, 30 μm wide, and 25 μm high; these numbers reflected the cell density used in our experiments and the worst-case scenario geometry. The boundary conditions included no-slip at the top and bottom surfaces, symmetry at the left and right boundaries, and defined parabolic velocity at the inlet and open outlet. In each simulation, the pressure drop in the channel, shear stress on the cell, and pressure on the cell were calculated. We estimated that with the mesh edge size we used (<0.5 μm), the error in shear calculation was <2%. (We performed one set of representative calculations with finer mesh sizes. The solutions converge and were used to compare to that of the coarser mesh used in most calculations.)

Design and Fabrication of Microfluidic Adhesion Devices. Using calculations and models as guidelines, we have designed two short-term devices (Figure 1A and B): the multisample device, which accommodates different surface chemistries or cell types, and the multishear device, which generates different shear stresses. We also considered nutrient and exogenous reagent delivery for longer-term cell incubation, in which nutrient depletion may be a critical issue. To provide continuous medium perfusion, a two-layer device was designed: the top layer consists of a bifurcated side-channel network for delivery into the main channel, which is in the bottom layer and where the cells reside (Figure 1C). Such a flow scheme ensures uniform delivery and minimizes shear stress during delivery. We estimated that, by diffusion alone, the mass-transfer time scale from the top to the bottom of the main channel (25 μm) was ~1−10 s ($D = 10^{-9}$−10^{-11} m^2/s), as compared to the average fluid residence time in the microchannel (~1 min).

The microfluidic devices were fabricated using PDMS rapid prototyping technique,[7] illustrated in Figure 2. Briefly, the photolithography masks bearing the designs were drawn using Freehand 9.0 (Macromedia Inc., San Francisco, CA) and printed on emulsion films with 5080 dpi resolution. The masters were created using a photopatternable epoxy (SU-8, Microchem Inc., Newton, MA) on silicon wafers using UV photolithography, and the PDMS elastomer devices were molded from the masters using two-part Sylgard 184 silicone elastomer (Dow Corning, Midland, MI). The details of a modified process for the two-layer long-term culture device are shown in Figure 2. Briefly, a first layer of SU-8 (2 μm) was spun, patterned using photolithography, developed only in the alignment mark areas, and cured on the silicon wafer, before a second layer (50 μm) was spun, aligned, and patterned. The two layers were subsequently baked and developed simultaneously. The masters were silanized using vapor-phase tridecafluoro-1,1,2,2-tetrahydrooctyltrichlorosilane (United Chemical Technologies, Bristol, PA) under vacuum before the PDMS was cured on them. Once cured, each PDMS device was punctured for inlet/outlet holes, treated with air plasma (100 mTorr at 18 W coil power for 30 s), bonded to a glass slide by placing the treated PDMS onto glass slides immediately after, and attached with

(12) Maheshwari, G.; Wells, A.; Griffith, L. G.; Lauffenburger, D. A. *Biophys. J.* **1999**, *76*, 2814−2823.
(13) Xie, H.; Pallero, M. A.; Gupta, K.; Chang, P.; Ware, M. F.; Witke, W.; Kwiatkowski, D. J.; Lauffenburger, D. A.; Murphy-Ullrich, J. E.; Wells, A. *J. Cell Sci.* **1998**, *111*, 615−624.
(14) Deen, W. *Analysis of Transport Phenomena*; Oxford University Press: New York, 1998.
(15) Happel, J.; Brenner, H. *Low Reynolds Number Hydrodynamics with Special Applications to Particulate Media*; Prentice-Hall, Inc.: Englewood Cliffs, NJ, 1965.

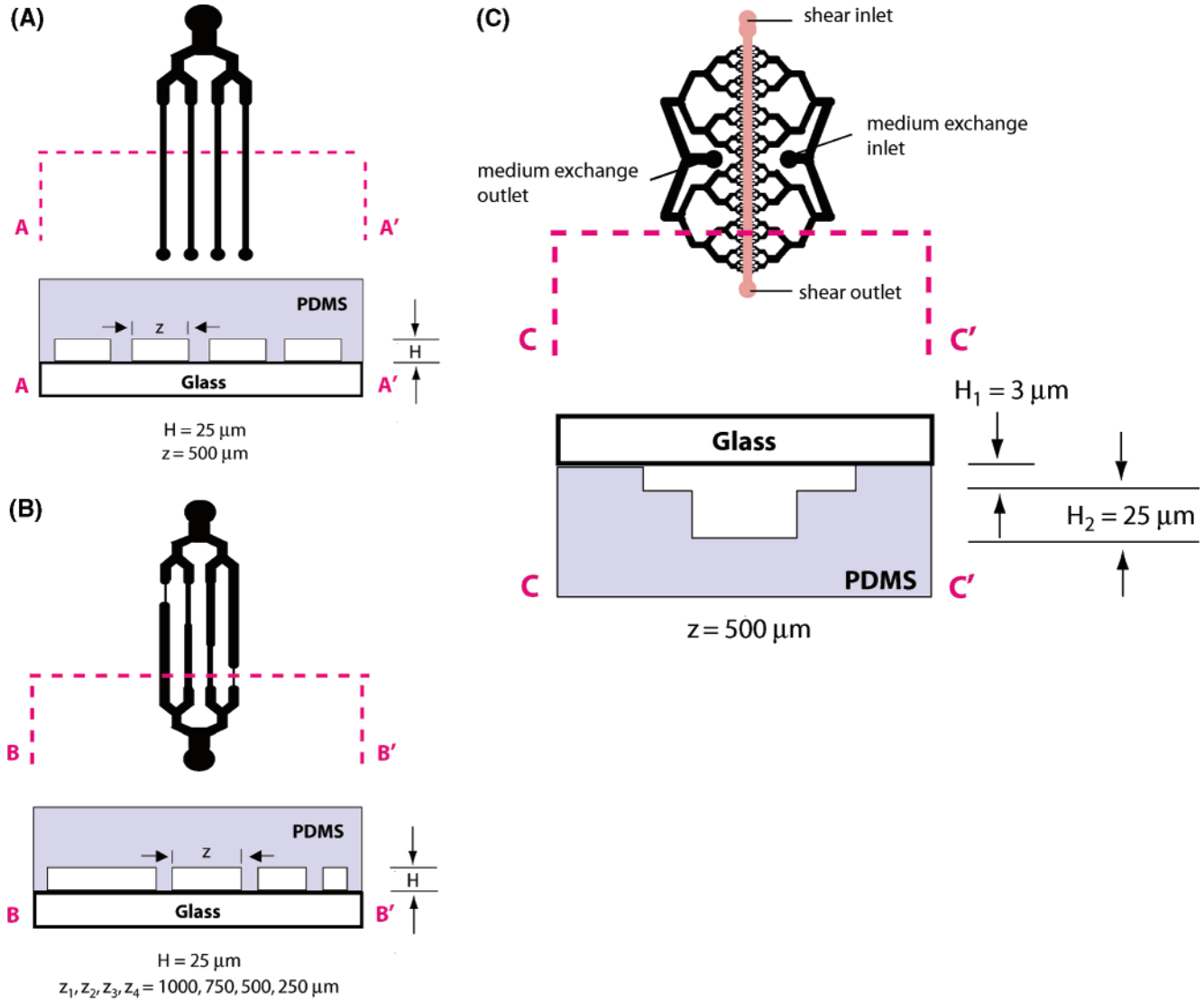

Figure 1. (A) Short-term adhesion multisample device accommodating identical channels (H = height; z = width). A−A′ is the cross-sectional view of the device. (B) Short-term multishear device has four channels with different width but same pressure drop. B−B′ is the cross-sectional view. (C) Long-term adhesion assay device has a two-layer design for uniform nutrient/reagents delivery (see text). The channel where cells reside is in pink. C−C′ is the cross-sectional view.

tubes. A second layer of PDMS was usually cast over the bonded devices and treated at 60 °C for 2 h to reinforce the mechanical stiffness of the PDMS device.

Cell Cultures. The fibroblast cell line WT NR6 is a gift from Alan Wells (U. Pittsburgh). It is a 3T3 variant that lacks endogenous EGF receptor (EGFR) but that expresses stably transfected human EGFR[16,17] and was routinely cultured in minimum essential medium-α (MEMα) supplemented with 7.5% fetal bovine serum (FBS), 350 μg/mL G418, 1 mM sodium pyruvate, 2 mM L-glutamine, 1 mM nonessential amino acids, 100 IU/mL penicillin, and 200 μg/mL streptomycin (Invitrogen, CA). Adhesion assay medium comprised MEMα with 25 mM HEPES supplemented with 1% dialyzed FBS and 1 mg/mL bovine serum albumin (BSA, Sigma, MO), with or without 100 nM human EGF (Sigma, MO).

Adhesion Assay. Prior to the assay, the microfluidic channels were sterilized with 70% ethanol and rinsed thoroughly with phosphate-buffered saline (PBS). Channels were then flushed with excess volumes of human plasma fibronectin (Gibco BRL) diluted in PBS (0, 0.1, 1, and 10 μg/mL), followed by physical adsorption of fibronectin onto the channel surfaces under static conditions for 1 h at room temperature. After rinsing with PBS, channel surfaces were incubated with 2% BSA for 1 h at room temperature to block nonspecific protein adsorption. All substrates were kept under PBS until cell seeding. WT NR6 cells were harvested using Versene (0.2% EDTA) to preserve integrin adhesion receptor integrity and delivered to the device at a cell density of 6×10^6/mL. In the short-term assays, cells were allowed to attach inside the microfluidic channel for 30 min at 37 °C in HEPES assay medium. Cell detachment was dynamically captured using time-lapse videomicroscopy. Briefly, a device seeded with cells was placed on a Ludl 99S008 motorized stage on a Zeiss Axiovert 35 microscope. At 4× magnification (~1.5 mm × 1,8 mm per field of view), three to four fields were selected from each channel (typically 30−150 cells per field) and images were acquired every 2 min using the OpenLab software (Improvision Inc., Boston, MA).

(16) Pruss, R. M.; Herschman, H. R. *Proc. Natl. Acad. Sci. U.S.A.* **1977**, *74*, 3918−3921.
(17) Chen, P.; Gupta, K.; Wells, A. *J. Cell Biol.* **1994**, *124*, 547−555.

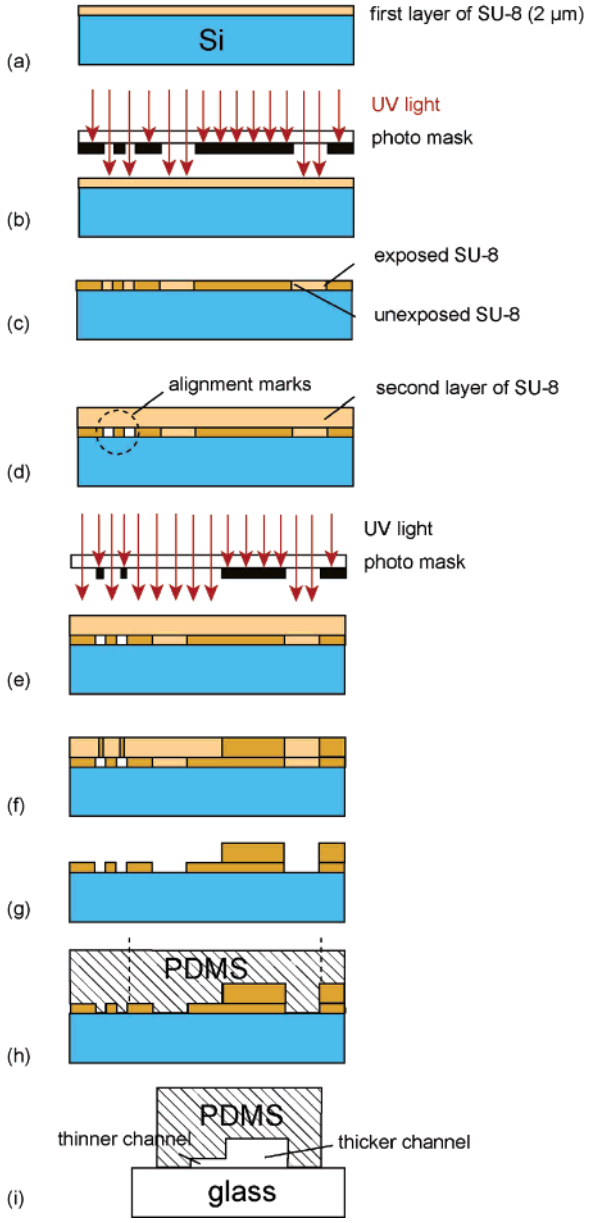

Figure 2. Fabrication processes used in the two-chamber perfusion microdevice for long-term shear assays. (a) Spin-coat the first thin layer with photopatternable epoxy (SU-8); (b) pattern the SU-8 layer with photolithography; (c) soft-bake the SU-8 to complete the cross-linking process and develop the un-cross-linked SU-8 around the alignment mark area; (d) spin-coat the second layer of SU-8; (e) align and pattern the second layer of SU-8; (f) soft-bake the wafer; (g) develop both layers of SU-8; (h) silane-treat the SU-8 master to prevent sticking and micromold PDMS polymer on the SU-8 master; (i) bond the PDMS to glass slide and assemble fluid connections. The single-layer devices (e.g., the short-term multisample and multishear devices) were fabricated using a similar process.

Because divalent cations are required for integrin−ligand binding, PBS containing calcium and magnesium were used as the shear buffer. Buffer flow rate was controlled using a Harvard Apparatus syringe pump (PH2000) at 1−10 mL/min depending on the experiments. Each experiment was repeated two to four times. The error bars represent the standard deviation of measurements from separate experiments. Cell detachment was quantified postassay. The fraction of adherent cells was determined as the number of cells remaining adherent at a given time divided by the number of cells before flow was applied. In the long-term assays, the device was inverted after seeding to allow cells to attach to the protein-coated (3 μg/mL fibronectin) PDMS surface[18] in the main channel, without entering the upper perfusion channels (Figure 5). Cells were incubated in HEPES assay medium for 1−2 h postseeding to allow cell attachment before the onset of perfusion. Medium was then delivered to the device via the bifurcated perfusion chamber at a rate of 2 μL/min for 10 h using a syringe pump. Cells were subsequently incubated in assay medium with or without 100 nM EGF for 1 h. The adhesion assay was conducted as described previously.

RESULTS AND DISCUSSION

Device Design and Fabrication. The design of the microfluidic cell adhesion devices was motivated by the following experimental objectives: systematic variation in ligand−receptor interactions, systematic variation in shear stress, study of short-term (<1 h or 30 min) as well as long-term (> 12 h) adhesions, and all these in the context of high-throughput assay performance. The designs exploit the available microfabrication techniques and advantages of the microfluidic systems.

The device design was guided by both analytical and numerical solutions of the laminar flow problems in confined channels. Figure 3A compares the different values of shear stress as a function of flow rate derived from the simple planar Poiseuille model to those of the 3-D analytical solutions for flow in rectangular pipes. To a first-order approximation, the simple model captures the shear stress characteristics in these microfluidic systems (accurate within 5%).

Both the analytical and numerical calculations demonstrate that more than 90% of the channel experiences a uniform shear stress distribution (<1% deviation) in the y direction (Figure 3B), consistent with the general observation that the wall effect persists within one height from the sidewall.[14] Therefore, in the designs with high aspect ratio, most of the cells are subject to a uniform shear stress. Accordingly, cells residing in the 5% edge area from each side of the channel were disregarded during postassay counting. Another related design requirement is to have fully developed flow under experimental conditions. The entrance length, i.e., the length it takes for the flow to become fully developed, is a function of *Re* (using the device thickness as the length scale): the larger the *Re*, the longer the entrance region.[19] For our experimental conditions, *Re* spanned from unity to a few hundred, depending on the flow rate.[14] Nevertheless, rule of thumb estimates as well as the above-mentioned numerical calculation of flow in empty channels showed that the entrance length was less than 1 mm, which was small compared to the length of the channel (10−20 mm). In the experiments, the entrance regions of the channel were excluded during image acquisition.

In the force estimation, we also considered the possible effect of cell topology. Olivier et al. and Gaver and Kute among others have examined the forces impacting on a cell in the Stokes flow.[20−22] The studies concluded that, in microscale, when the ratio

(18) Anderson, J. M.; Ziats, N. P.; Azeez, A.; Brunstedt, M. R.; Stack, S.; Bonfield, T. L. *J. Biomater. Sci. Polym. Ed.* **1995**, *7*, 159−169.
(19) McIntire, L. V.; Frangos, J. A.; Rhee, B. G.; Eskin, S. G.; Hall, E. R. *Ann. N. Y. Acad. Sci.* **1987**, *516*, 513−524.
(20) Olivier, L. A.; Yen, J.; Reichert, W. M.; Truskey, G. A. *Biotechnol. Prog.* **1999**, *15*, 33−42.
(21) Olivier, L. A.; Truskey, G. A. *Biotechnol. Bioeng.* **1993**, *42*, 963−973.

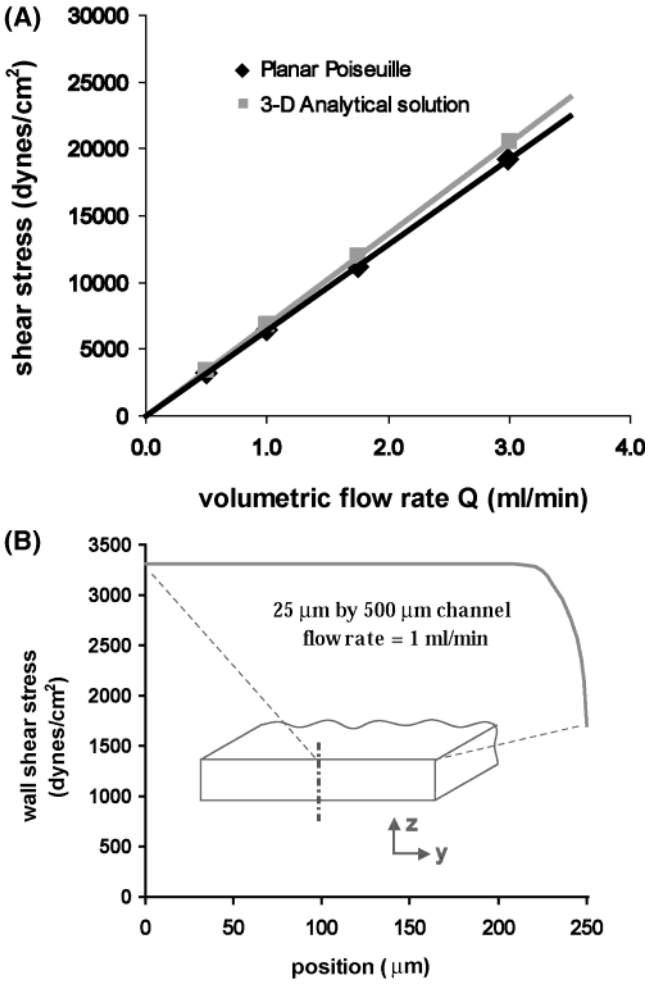

Figure 3. (A) Comparison between the planar Poiseuille model and the 3-D analytical solution to flow in rectangular pipes. The stress calculation derived from the planar model is a good approximation of the actual wall stress in a device with large aspect ratio. (B) The stress distribution in the $y-z$ cross section of the microchannels.

of cell dimension to channel dimension is not low, the actual shear stress felt by the cells could be significantly different from the wall shear stress because of a nonnegligible distortion of the flow by the cell. Because the force calculation seems to be highly sensitive to the actual geometry, we employed 3-D numerical simulations to compute the shear force on the cell surface as well as the pressure force on the body of a cell with prespecified 3-D geometry. The presence of a nonflat cell in the microchannel changes the velocity distribution and correspondingly the shear stress and pressure distributions (Figure 4A). The top of the cell dome experiences higher shear stress than the edge, but the average shear stress is comparable to that corresponding to an empty channel (top figure). There is also a significant pressure force acting on the cell in the direction of the flow (bottom figure). This pressure effect was sensitive to *Re* (flow rate) because the distortion in the velocity field gave rise to the drag force and the flow was no longer unidirectional (Figure 4B). These observations were in agreement with the conclusions from the studies by Gaver and Kute.[22]

The present simulations did not capture the dynamic changes in cell shape. In principle, more information on the exact shape and dimensions of the cells can be extracted from microscopy images at any given time during the experiments and then used as input to calculate the exact force, as Olivier et al. have demonstrated.[21] For the work presented in this paper, we envision that most applications of this assay will be comparative studies in which the calculations provided here would be sufficient.

Cell Adhesion on Varying Protein-Coated Surfaces. The multisample microfluidic device has channels that allowed multiple conditions to be examined in one experiment while maintaining the same shear stress. The identical dimensions of each channel on a single device as well as the fidelity of channel dimensions from device to device ensured that the same shear stress was maintained in all channels. Fibronectin was used as a prototype ECM protein. Each of the four channels was coated with fibronectin molecules from solutions of 0, 0.1, 1, and 10 μg/mL, respectively; shear stress was increased from 0 to 1600 dyn/cm^2 through step increases in the buffer flow rate at discrete time intervals to sample increasing levels of force response. This experimental scheme is recommended for conducting initial experiments in order to locate the relevant detachment force range for a new cell/substrate system. We found that cell adhesion strength depended on fibronectin surface density (Figure 5). At the highest fibronectin density (corresponding to a coating concentration of 10 μg/mL fibronectin), barely 10% of the cells seeded in the channel were detached at the end of the experiment. In contrast, at the lowest ligand density (0.1 μg/mL coating density), nearly all cells were removed shortly after a small shear force was introduced. As expected, at the intermediate coating concentration (1 μg/mL), cells exhibited a gradual detachment profile as the shear stress was increased. Such dependence of WT NR6 adhesion strength on fibronectin surface density has been observed before using the centrifugation assay.[23] However, the fibronectin coating concentrations sampled were usually limited to less than 1 μg/mL in order for the cells to be susceptible to the detachment forces allowed by the centrifuge. This multisample device has been also used to measure and compare the adhesion strength of a parental cell line and its cytoskeletal mutants (data not shown). Furthermore, the force range (0−1600 dyn/cm^2) used in the experiment is well within the capability of our device. We describe in the subsequent sections that the microfluidic devices can detach cells at higher fibronectin density (e.g., 10 μg/mL) as well as after they have been cultured overnight.

Cell Adhesion with Varying Shear Stresses. The next design objective was to create an array of channels that could offer different values of time-invariant shear stress in a high-throughput fashion. In conventional approaches such as centrifugation or parallel plate assay, it is not possible to sample more than one force at a time. The radial flow assay and the parallel plate assay with tapered channels allow simultaneous sampling of different force conditions, but the continuous change in geometry and variability of device thickness during assembly complicate exact force determination. In our study, the multishear device achieved built-in variation in shear stress across the channels by giving each channel a different width while maintaining identical pressure drop by compensating the length of the channels. For example,

(22) Gaver, D. P.; Kute, S. M. *Biophys. J.* **1998**, *75*, 721−733.

(23) Koo, L. Y.; Irvine, D. J.; Mayes, A. M.; Lauffenburger, D. A.; Griffith, L. G. *J. Cell Sci.* **2002**, *115*, 1423−1433.

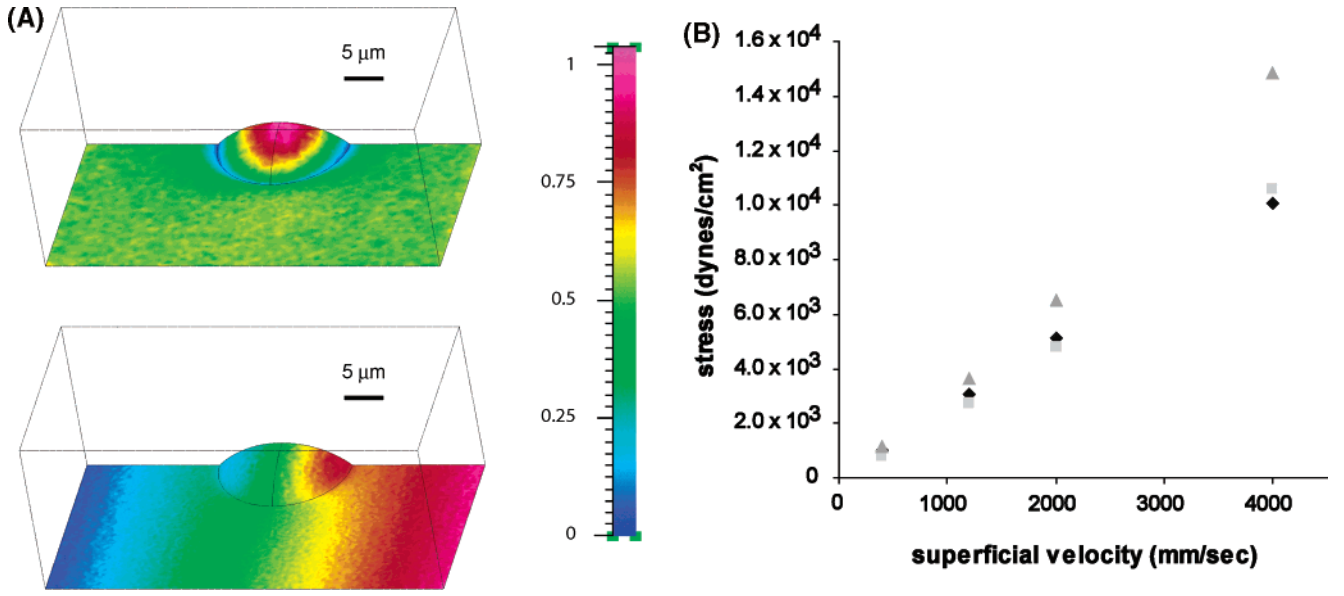

Figure 4. (A) 3-D numerical calculation of force showing that the apex of the cells experiences most of the shear forces (top figure) while the basal areas near the bottom wall of the microchannels experience much less shear force the pressure forces acting in the direction of the flow (from right to left) (bottom figure). (B) Comparison between shear stress experienced by a protruding cell (3-D numerical model), and wall shear stress (3-D analytical solution). Diamond, shear stress on the flat surface; square, shear stress on a dome-shaped cell; triangle, sum of pressure and shear stress on the dome.

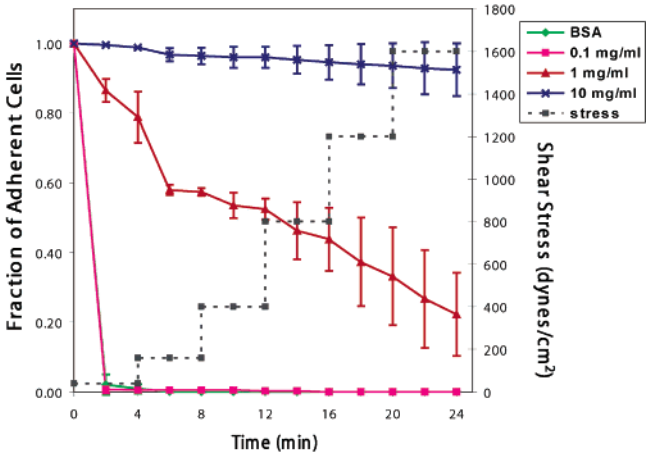

Figure 5. Effect of fibronectin coating concentration studied using the multisample device. Diamond, channels coated with BSA only; square, 0.1 μg/mL fibronectin; triangle, 1 μg/mL fibronectin; cross, 10 μg/mL fibronectin; dotted line, nominal shear stress.

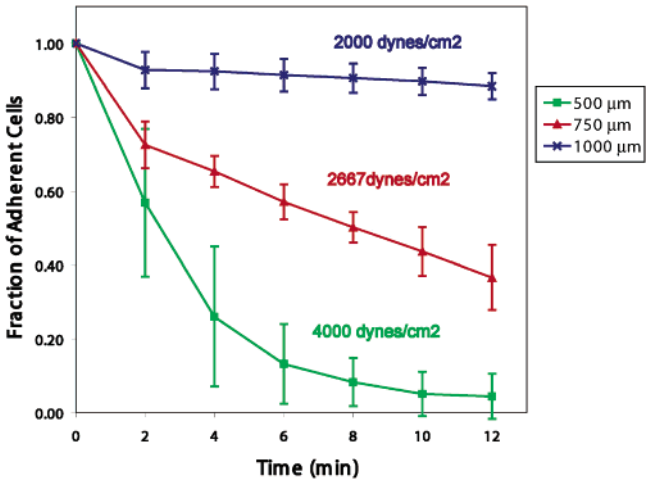

Figure 6. Effect of time-invariant shear stress studied using the multishear device. Channels widths: square, 500 μm; diamond, 750 μm; cross, 1000 μm.

when channel width was narrowed from 1000 μm to 750 μm and to 500 μm, the length was shortened accordingly; and a 1.5- and 2-fold increase in shear stress, respectively, was effectively introduced. Previous experiments using the multisample device showed strong cell adhesion on a 500-μm-wide channel coated with 10 μg/mL fibronectin, with only ~10% of cells distracted at the maximal shear stress value of 1600 dyn/cm^2. To capture the dynamic cell detachment profile effectively, much higher shear stress must be applied. Thus, a constant flow rate of 1.25 mL/min per channel was selected and applied throughout the experiment using the multishear device to maintain time-invariant, but channel width-dependent, shear stress in channels with 500, 750, and 1000 μm in width, yielding shear stress values of 4000, 2700, and 2000 dyn/cm^2, respectively. With these relatively high levels of shear stress, different cell adhesion profiles were obtained in the high adhesion regime (10 μg/mL fibronectin), as illustrated in Figure 6. At a shear stress level of 2000 dyn/cm^2 applied for 12 min, only ~10% of the cells detached, but with a 2-fold higher shear stress, greater than 90% of the cells came off the surface during the same time period. An intermediate adhesion profile was obtained at an intermediate shear stress. The linear detachment profile suggested that 2700 dyn/cm^2 was a force regime to which most of the cell population was susceptible; therefore, it provided the most dynamic detachment kinetics under the given conditions. On the other hand, 80% of the cells came off the substrate within the first 4 min when the shear stress was increased to 4000 dyn/cm^2. Therefore, this force regime captured only the detachment dynamics of a small and highly adhesive population from the cell adhesion histogram. In one experiment, the multishear device can effectively identify the force−response regime of a cell population of interest rather than introducing stepwise changes in buffer flow rate as we did in the previous

section. Thus, the multishear device can provide a systematic approach to varying shear stress, determining the force level that is most relevant for the adhesion measurement of a cell population of interest, as well as performing the kinetics study of these population events.

Long-Term Shear Assays. Nutrient and Reagent Delivery. Long-term cell adhesion is rarely quantified, in part because of the large forces required to detach well-adherent cells such as fibroblasts. For example, using a spinning disk device, Garcia et al. showed a 10−20 times increase in adhesion strength after IMR-90 fibroblasts were plated overnight on 2 μg/mL fibronectin surfaces.[24] However, a conventional parallel plate device has typical cross-sectional dimensions on the order of 1 mm × 1 mm, which would require unrealistically high flow rates to remove adherent cells. Similarly, using a commercial supercentrifuge, the centrifugation assay could not dislodge cells as soon as 15 min after seeding at 37 °C,[25] or very low fibronectin densities must be used to allow detachment of strongly adhesive cells.[23] As demonstrated in the previous sections, microfluidics may provide a solution to such limitations; however, the small dimensions now pose a challenge to adequate nutrient deliver. A typical microfluidic channel holds a total volume on the order of 1 μL. Thus nutrient delivery and medium exchange become critical in maintaining long-term cell viability. As illustrated in Figure 7A, when cells were incubated in the long-term device for 12 h without perfusion on 10 μg/mL fibronectin, many of the cells rounded up or had fragmented cell membranes, indicative of unhealthy or dying cells. In addition to the material exchange concern, it is conceivable that nucleation of gas bubbles is more facile in microdevices because of the large surface area-to-volume ratio and the accumulation of cellular debris. To address these issues, a dual-chamber perfusion design is introduced to allow cell adhesion quantification after overnight incubation and to improve nutrient and gas exchange within the microchannels. These perfusion networks can also be used to deliver exogenous reagents uniformly throughout the channel, thereby allowing biochemical studies. Moreover, the shear stress introduced during medium delivery from the bifurcated channels is minimal (<0.05 dyn/cm^2). The dual-chamber design also prevents cells from moving into the bifurcated network to interfere fluid distribution. When fresh assay medium was delivered at a rate of 2 μL/min, cells continued to spread and retained an appearance that was similar to those cultured under macroscopic conditions (Figure 7B), and no bubble generation was observed under the flow conditions.

Cell adhesion is regulated not only through adhesion to the matrix proteins but also through soluble molecules. For example, EGF has an established role in the disassembly of focal adhesions, thereby reducing cell adhesion.[12,13,26] Studying the effects of EGF usually involves an extended period of serum deprivation to return EGF signaling to the basal level, which is then followed by EGF stimulation. Using the perfusion device, WT NR6 fibroblasts were serum-starved for 12 h inside channels coated with 3 μg/mL fibronectin. The perfusion chamber then uniformly delivered EGF

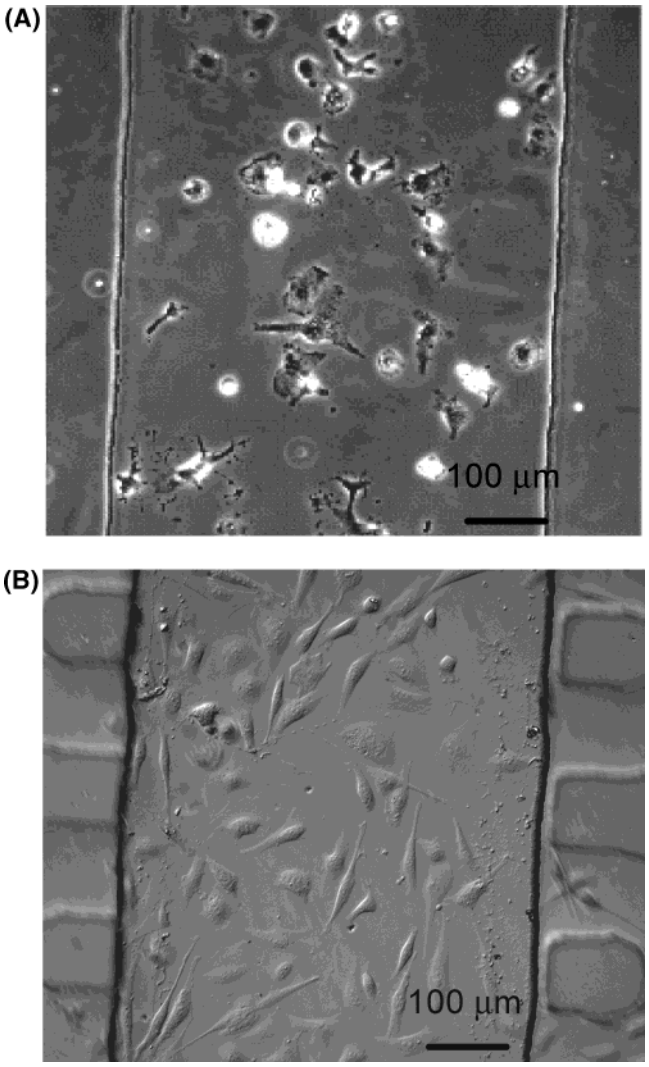

Figure 7. (A) Without medium replenishment. WT NR6 cells did not survive a 12-h incubation in the microchannels. (B) With continuously medium perfusion. Cells remained viable and healthy after a 15-h culture in the long-term device.

to the main channel. After 1 h of treatment, the weakening effect of EGF on cell adhesion was clearly demonstrated in Figure 8. The majority of the treated cells were removed after a shear stress of 6400 dyn/cm^2 was applied for 3 min. The control population exhibited higher resistance to shear, with 10% of which remained attached after the same stress was applied for 9 min. It should be noted that we were able to fully remove spread fibroblasts at the end of the assay by applying ~6000 dyn/cm^2, using a flow rate that was well within the technical limit of the system. This threshold of detachment force was comparable to the 2500 dyn/cm^2 shear stress reported by Garcia et al. using the IMR-90 fibroblasts[24] and was in agreement with the theoretical calculation of ~6000 dyn/cm^2 by Olivier and Truskey.[21] Furthermore, the results also demonstrated the importance of employing quantitative methodology in addressing biological phenomena. For example, without knowing the relevant detachment force range for the cell population of interest, the adhesion strength of EGF-treated and untreated cells appeared to be similar when only a small shear stress was applied. This would have been misleading since 1500 dyn/cm^2 was apparently below the threshold detach-

(24) Garcia, A. J.; Takagi, J.; Boettiger, D. *J. Biol. Chem.* **1998**, *273*, 34710−34715.
(25) Lotz, M. M.; Burdsal, C. A.; Erickson, H. P.; McClay, D. R. *J. Cell Biol.* **1989**, *109*, 1795−1805.
(26) Lu, Z. M.; Jiang, G. Q.; Blume-Jensen, P.; Hunter, T. *Mol. Cell. Biol.* **2001**, *21*, 4016−4031.

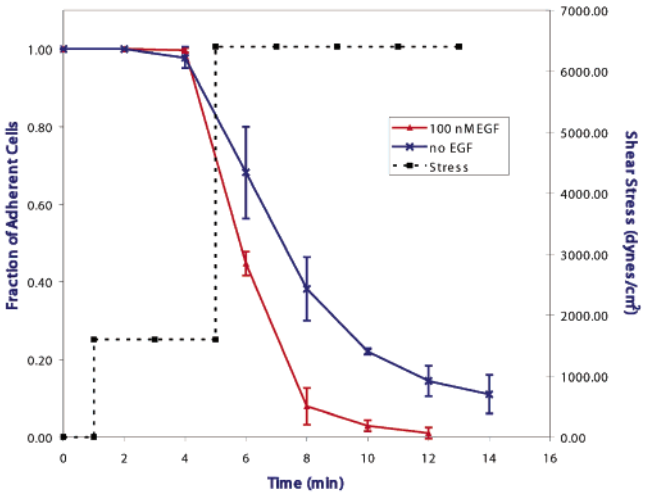

Figure 8. A 12-h period of quiescence in the long-term device. Following quiescence, WT NR6 cells were treated with 100 nM of EGF, which was delivered through the perfusion network. Triangle, EGF-treated cells; cross, control cell; dotted line, nominal shear stress.

ment force for either cell samples. At a higher shear stress, the difference between the treated and control populations became evident.

In these experiments, we successfully cultured fibroblasts for long-term biochemical and biomechanical studies on cell adhesion in microchannels. The microfluidic assays properly identified the appropriate detachment force range and clearly demonstrated the de-adhesive effects of EGF that has been observed using conventional methods.[12,13] Furthermore, the assay achieved adequate shear stress to remove fully spread cells. It is conceivable that these devices can be incorporated as an upstream component to other microdevices that perform subcellular and molecular analysis, such as identifications and quantifications of the signaling molecules.[27]

CONCLUSIONS

Exploiting the unique properties of microfluidics, we have demonstrated high-throughput experimentation on cell adhesion determination. The multisample and multishear devices were representative of the prototype designs used to demonstrate and validate the working principle of microfluidic cell adhesion assays. Because of the small dimensions, it was possible to achieve large shear stress while preserving laminar flow. Studies of time-dependent and soluble factor-dependent cell adhesion phenomena were also made feasible. The high-throughput testing and amendable design of these devices would allow efficient assessment of various regulative mechanisms for cell adhesion by introducing multiple changes to the extracellular environment in one experiment. The applications of such devices can be broadened to other cell-based biological assays, such as cell migration and mechanotransduction.

ACKNOWLEDGMENT

We thank the DARPA Bio-Info-Micro Program (MDA972-00-1-0030), the NIH Cell Migration Consortium (NIH GC10641), the NSF graduate fellowship to H.L., and the Whitaker Foundation graduate fellowship to L.Y.K. for financial support, and the technical staff of the Microsystems Technology Laboratories at MIT for technical assistance.

APPENDIX

The analytical expression represents the linear velocity, u, in terms of the spatial coordinates (x the flow direction, y the wall-wise direction, and z the span-wise direction)

$$u = -\frac{\Delta p}{2\mu l} y(y-h) + \sum_{m=1}^{\infty} \sin\left(\frac{m\pi y}{h}\right)\left(A_m \cosh\frac{m\pi z}{h} + B_m \sinh\frac{m\pi z}{h}\right) \quad \text{(A1)}$$

where

$$A_m = \frac{h^2 \Delta p}{\mu m^3 \pi^3 l}(\cos m\pi - 1), \quad B_m = -\frac{A_m(\cosh m\eta\pi - 1)}{\sinh m\eta\pi}, \quad \text{and } \eta = \frac{w}{h}$$

The shear stress at the wall is the derivative of u with respect to position y evaluated at $y = 0$, i.e.

$$\tau_w = -\mu \frac{du}{dy}|_{y=0} = \mu\frac{\Delta p}{2\mu l}\left(\frac{1}{2}y - h\right) - \mu\sum_{m=1}^{\infty}\left(\frac{m\pi}{h}\right)\cos\left(\frac{m\pi y}{h}\right)\left(A_m \cosh\frac{m\pi z}{h} + B_m \sinh\frac{m\pi z}{h}\right) \quad \text{(A2)}$$

The pressure drop is determined from the total flow rate (Q) by integrating the velocity expression with respect to y and z:

$$\frac{\Delta p}{l} = Q \Big/ \left[\frac{1}{24\mu} hw(h^2 + w^2) - \frac{8}{\pi^5 \mu}\sum_{n=1}^{\infty}\frac{1}{(2n-1)^5} \times \left[h^4 \tanh\left(\frac{2n-1}{2h}\pi w\right) + w^4 \tanh\left(\frac{2n-1}{2w}\pi h\right)\right]\right] \quad \text{(A3)}$$

The infinite sums converged quickly and were truncated when the convergence criterion

$$\left|\frac{1}{(2N-1)^5}\left[h^4 \tanh\left(\frac{2N-1}{2h}\pi w\right) + w^4 \tanh\left(\frac{2N-1}{2w}\pi h\right)\right]\right| < \xi \sum_{n=1}^{N-1}\frac{1}{(2n-1)^5}\left[h^4 \tanh\left(\frac{2n-1}{2h}\pi w\right) + w^4 \tanh\left(\frac{2n-1}{2w}\pi h\right)\right] \quad \text{(A4)}$$

was satisfied, where ξ is a small number ($<10^{-5}$).

Received for review January 28, 2004. Accepted July 2, 2004.

AC049837T

(27) Lu, H. Ph.D. thesis, Massachusetts Institute of Technology, Cambridge, MA, 2003.